Revised Manuscript (Clean, unmarked, FINAL version)

A fuel cell powered autonomous surface vehicle: the Eco-SWAMP project

V. Boscaino[*], A. Odetti[**], G. Marsala[*], D. Di Cara[*], N. Panzavecchia[*], M. Caccia[**], G. Tinè[*]

[*] Institute of Marine Engineering, National Research Council of Italy, via Ugo La Malfa, 153 – 90146 Palermo, ITALY.

[**] Institute of Marine Engineering, National Research Council of Italy, Via De Marini 6 -16149 Genoa, Italy

Corresponding author: Valeria Boscaino, Institute of Marine Engineering, National Research Council of Italy, via Ugo La Malfa, 153 – 90146 Palermo, ITALY. E-mail: valeria.boscaino@cnr.it.

Abstract – Autonomous surface vehicles are becoming consolidated robotic tools for marine, coastal and inland surveys. Autonomous surface vehicles are usually equipped with electronic instruments to perform remotely controlled or autonomous geo-morphological, biological, chemical, physical analyses and data collection. Actually, well-established solutions provide battery power but the research focuses on introducing a fuel cell to decrease the environmental impact meanwhile increasing the cruising range. In this paper, the design of the Eco-SWAMP, a fuel cell powered autonomous surface vehicle, is presented starting from its battery-powered version, the SWAMP prototype. The experimental power consumption profile of the SWAMP during four missions is analysed to define the primary energy sources ratings of the Eco-SWAMP. After a commercial choice of primary sources, power management algorithms are designed and compared in MATLAB/Simulink environment by simulation results. The proposed procedure can be easily applied to any autonomous marine vehicle.

Keywords: fuel cell, hydrogen energy, autonomous marine vehicle, fuel cell powered vehicles, power management algorithms, power converters.

1. Introduction

Nowadays, the Unmanned Vehicles (UVs) are widely used for missions of surveillance and monitoring in several applications, such as industrial, scientific, military and security [1]. In particular, in the ocean explorations, due to their safety and versatility, the UVs mark a new beginning in the way the sea is explored and studied. In the marine applications, Unmanned Marine Vehicles (UMVs) can act in a remotely controlled, semi-autonomous or autonomous way, thus reducing or nulling any human interaction. Moreover, they can operate underwater or on the surface thus allowing to explore aquatic environments, that would be dangerous for human crew, and to extend the operations to inaccessible areas [2]. In case of autonomous or semi-autonomous vehicles, Autonomous Marine Vehicles (AMVs) can act on the surface as Autonomous Surface Vehicles (ASVs) or underwater as Autonomous Underwater Vehicles (AUVs). The AMVs can be developed with a great variety of equipment, thus becoming very versatile to carry out different types of missions. In the scientific research, AMVs are used for a wide variety of surveys like water sampling and monitoring of biological, chemical and physical parameters [3,4], bathymetries [5–7], underwater structure monitoring [8], hydrographic and geomorphological data [9], aquaculture [10], earthquake prediction [11], marine archaeology [12,13] and air atmosphere measurements [14]. In the military missions, the AMVs allow to carry out maritime security, the electronic and surface warfare, the mine countermeasures and the maritime interdiction operations. Moreover, the AMVs can be used for offshore works, like shipwreck survey, structure inspection, communication, online data monitoring and subsea pipeline. Nowadays, because of the several scientific missions and aquatic environments, a great variety of these kinds of vehicles has been produced by the civil industry with different sizes and hull types. In fact, the mission requirements and environmental conditions affect the size and the choice of the hull type. The requirements include the endurance, the nominal speed, the maximum depth and the required payload to complete the mission [15]. The ASVs, for example, can be a mono-hull or a multiple-hull like catamaran or small water plane area twin hull or multi-maran. Each mission also requires different kind of equipment, which can be divided into the basic and the mission

equipment. In the basic equipment, there are the propulsion system, the energy generation and storage system, the navigation guidance and control (NGC) and the communication systems. The mission equipment, like sonar and sensors, changes with the specific mission requirements. This equipment can affect the payload of the vehicle because of its weight and volume. Although today the electronic devices are smaller and lighter, the weight of the vessel is increased by the weight of the energy/storage system, which limits the autonomy of the AMV and therefore the endurance of the mission [16]. Current commercial AMVs use lead-acid or Li-ion batteries for energy storage [17]. Moreover, a mother ship that gives information during the navigation follows most AMVs. After the mission, the ship must recover the AMV or connect it to a docking system for the recharging and the data download. In order to reduce the need of the mother ship and therefore the cost of the mission, it is necessary to develop a long-endurance AMV. This goal can be achieved by new solutions for the power supply and the storage systems, which affect the AMVs working duration and mission completion. The standard power system, currently used in AMVs, is based on secondary batteries (lithium-ion), which are a simple and relatively inexpensive solution. These batteries can be recharged and used for many times with a long operation life [18]. Since this technology has reached a mature state, in spite of the efforts of the scientists to increase the energy density, the current Li-ion battery technology remains the best choice for the near to mid-term future [19,20]. By increasing the AMV endurance would imply increasing the volume and weight. In order to increase the mission endurance of the AMVs powered by batteries, it is necessary to use high capacity batteries, which are usually characterized by high size and weight. This can represent a very strong limitation in the design of the lightweight ASVs, where the size and the weight of the vessel are very stringent constraints. The energy density, defined as the amount of energy per unit mass or volume, represents the most significant parameter, giving a measure of the system trade-off between weight, size and energy and endurance performances. For this reason, energy sources with a high energy density represent a very promising solution. Therefore, a power source with high storage energy density for lightweight ASVs should be identified. For this application, the power source must comply with some constraints: a

small acoustic signature, in order to perform precise and accurate sonar readings, and a small thermal signature, in order to avoid interferences with other sensors affected by the temperature. A possible solution is represented by the Fuel Cells (FCs) for their capability of achieving higher energy densities than those offered by the batteries. In [20], a review study comparing different storage technologies and sources including Li-ion batteries and PEM fuel cells is presented. In this study, energy density, power density, specific power and energy, efficiency, lifespan and cost are accounted for. In particular, the cited paper reports a 400kWh/m^3 energy density for a PEM fuel cell and a 280kWh/m^3 energy density for a Li-ion battery.

In the last few years, institutions and scientists have made great efforts to increase the endurance and the range of AMVs, without increasing their size too much, by means of fuel cells [21–25]. In [21], the authors developed a hydrogen storage system for portable/mobile applications, such as unmanned underwater vehicles. A new system integration strategy has been implemented in order to maximize the energy density of the system, including the electrolyser, a metal hydride tank and a PEM fuel cell. In [22], the authors compared several power sources for AUVs. The work showed that the use of batteries for deep diving vehicles is advantageous if ambient pressure is considered. Moreover, the authors asserted that for deep diving survey applications and in the near future, the fuel cells will be more attractive than batteries for their light weight, rapid refilling and high efficiency. [23] is a comprehensive review of the state of art on the applications of Fuel Cells (FCs) in maritime applications. In particular, the authors compared several projects described in the existing literature, and several kinds of FCs have been proposed to power ships or sea vehicles. The authors highlighted that, for small and medium applications, low temperature FCs, such as PEMFC, are more suitable than high temperature FCs. Moreover, the paper asserts that, although the scientists have made several efforts to meet the environmental constraints, the integration of fuel cells into commercial ships or AMVs requires overcoming other critical issues, such weight and volume of FCs, dynamic of ship, reforming of fuel and atmosphere composition. In [24], the authors presented a report of technical and economic feasibility of a coastal research ship powered by a PEM fuel cell in standalone

configuration. In order to design a vessel oriented to science missions, as coastal oceanography, a feasibility analysis was carried out. The hull shape analysis shows that the trimaran can satisfy the space and volume constraints required for a proper vessel operation. Moreover, the report highlights that with the integration in the vessel of a 1800 kW PEM FC for primary propulsion and 10,900 kg of consumable stored hydrogen is possible to complete a mission of 2400 nautical miles with an average cruising speed of 10 knots. By using hydrogen-fed renewable power sources, the predicted annual emissions are 91.4% less than those of an equivalent ship powered by conventional diesel engines. The authors estimated that the cost of the PEMFC-powered ship is 7.7% higher than the equivalent diesel vessel, where the hydrogen is made from fossil natural gas or steam reforming. [25] is a review of the project and studies on application of the FCs on surface vessels and submarines. The authors compared the different fuel cell technologies for marine applications in terms of operating temperature, energy density, weight, size and cost. The paper highlights that PEMFCs are not yet a mature technology for military and civilian marine applications unlike the submarines. Moreover, the authors asserted that the possibility to use the available commercial fossil fuel, instead of the pure hydrogen, is an open research topic and challenge of fuel cell applications on commercial ships. This solution can be implemented by using an on-board fuel reformer to extract the hydrogen from the marine fuels, such as diesel oil or methanol.

A fuel cell is a zero CO_2 emissions device that converts fuel and oxidant directly into electricity by an electrochemical process with high efficiency [26]. The basic fuel cell can generate electricity silently because it has no moving parts, it needs low maintenance with a long operation time and it is very eco-friendly [27]. Unlike the batteries, the chemical reactants are continuously supplied by an external storage system. The fuel cell outperforms the energy density of batteries because of the peculiar features of the fuel storage. For instance, the mass of hydrogen FCs can be three times lower than that of the lithium-based battery being the same as the stored energy [28]. Concerning the cost of batteries and fuel cells, the mission endurance is a key factor to account for. In particular, for automotive applications, the cost of the battery-powered vehicles increases quickly with the cruising

range. This depends on the use of a high capacity battery, featuring high cost. Although the fuel cell price increases with its power size, this cost changes with the mission duration much lower than the battery ones. In fact, the consequent increase in the hydrogen storage has a low impact in the overall fuel cell system cost [29]. In [21], a comparison in terms of lifespan is made and batteries outperforms PEM fuel cells. The degradation of the battery depends on several aspects, such as the chemical composition, the quality of manufacturing materials, the cell packaging, loads, charging patterns and thermal conditions. The fuel cell lifespan is significantly affected by the loading pattern. In particular, the on/off cycling represents the main reason for the fuel cell degradation (up to 94%) [30]. Therefore, the power management algorithm can improve the lifespan of the PEM fuel cell by reducing the number of on-off cycles and power transitions. The size of a standalone fuel cell system is dimensioned to match the power demand of the application, while the external fuel storage system is dimensioned to match the energy demand. There are several fuel cells depending on the electrolytes, phosphoric acid fuel cell (PAFC), molten carbonate fuel cell (MCFC), solid oxide fuel cell (SOFC), polymer electrolyte fuel cell (PEFC) and proton exchange membrane fuel cell (PEMFC) [25]. They differ in terms of operating temperature, fuels and exhaust heat utilization. PEMFC and PEFC fuel cells represent the best choice for powering the AMVs for several reasons: the highest operating temperature of PEFC and PEMFC is about 80 °C and 60-80 °C, respectively; the fuels are accessible, such hydrogen and natural gas; the fuel cells are easy to start and stop; exhaust heat utilization is safe, just hot water, and very high power density. In particular, since the PEMFC is actually the most common fuel cell type and the technology is mature and robust, these kinds of fuel cells began to be applied in some AMVs, even for their low environmental impact [22–25,31]. In 1998, the Japan Agency for Marine-Hearth Science Technology (JAM-STEC) developed the world's first AUV "Urashima" powered by PEFC fuel cell [28]. In 2005, the AUV performed a 56 hours mission, reaching 317 Km length and 800 m of depth with an energy efficiency of 60%. In 2004, the German Federal Ministry for Education and Research (GFMER) funded a hydrogen AUV called "DeepC" [32], which performed a 60 hours endurance mission. The lack of FCs in commercial AMVs is mainly

due to the high cost of this technology at its current state. However, in the following years, the price of this technology is expected to go down and a first generation of commercial FC AMVs will be released. Although the PEMFC is one of the advanced power sources for AMVs vehicles, it has some drawbacks, such as a long start-up time [33] and a slow power response [34]. Moreover, if the electric propulsion system of AMVs is equipped with a fuel cell only, the dynamic response of the power system will be affected by the slow transient response of the fuel cell itself. For these reasons, the hybridization of the PEMFC with other power sources, such as batteries or supercapacitors, represents an effective solution to overcome drawbacks. The main advantages brought by hybrid fuel cell/battery power systems with respect to stand-alone batteries or fuel cells relies on higher specific energy and a redundancy in power supply. Therefore, the system performances are increased because the probability of energy failures are limited. If compared to standalone configurations, the hybrid power source features smaller size and higher efficiency. In the literature, hybrid power systems can be classified into two types: direct (passive) and indirect (active) hybrid configurations [35]. The choice of the configuration depends on the AMV power and energy requirements, battery ratings, fuel cell characteristics, weight and volume constraints. The direct hybrid construction directly connects the power sources to the DC bus or load without any DC-DC conversion or regulating system. The indirect configuration allows a precise control of the power system by means of DC/DC converters. The main drawbacks brought by an active configuration are the complexity of the topology, higher weight, volume and voltage losses, which contribute to a reduced efficiency. Although the direct hybrid configuration features lower losses, simple architecture and reduced cost, the active power control is not allowed. For this reason, an external control system is usually required to regulate the operating conditions of the batteries and/or the fuel cell. Research actually focuses on the hybrid fuel cell/battery power system for AMVs [36–43]. In [36], an active hybrid polymer electrolyte fuel cell / lithium ion battery system for a lightweight AUV is presented. The analysis is based on the size and weight of the system components. A comparison with battery and fuel cell standalone configurations is performed. The impact of hydrogen and oxygen storage tanks on the mass and volumetric

constraints of the AUV under test is analysed. Several hydrogen storage technologies are compared to identify a viable solution for the mission endurance ratings. In [37], the importance of the fuel cell as a zero-emission source is outlined. A simulation model of an active fuel cell – battery hybrid power system of an unmanned aerial vehicle, including the fuel cell model and the full load power consumption, is presented. For the energy management system, a rule-based state-machine strategy is adopted. The proposed simulation platform, including the full load power consumption of the aerial vehicle, allows the designer to test the fully functionality of the energy management system. In [38], a fuel cell sizing tool for AUVs is presented. The proposed sizing method allows the designer to size the fuel cell ratings and weight in order to power an AUV. A comparison between three different solutions in terms of weight, volume and energy density is performed: hybrid battery fuel cell, fuel cell alone and battery alone. Several hydrogen and oxygen storage technologies are compared in terms of weight and volume of the final power system. As a result, if large energy amounts are required, the hybrid system with well-selected storage technologies will be more volume-efficient. If short missions are accounted for, standalone batteries become more attractive because of the reduced complexity and volume constraints of the standalone configuration. Yet, the actual trend is to enlarge autonomous vehicles freedom from the main docking station, thus pressing for longer and longer mission endurances. In [39], the design of a small ASV power system based on an wind-solar storage and fuel cell/battery hybrid energy supply is presented. Elements affecting the ASV power system are accounted for. In [40], a passive hybrid power configuration for an Unmanned Ground Vehicle (UGV) based on a direct coupling between the fuel cell and the Lithium-ion battery is proposed. Advantages and drawbacks of active and passive hybrid configurations are reviewed and several passive hybrid configurations are presented. The power consumption profile is heavily dependent on the driving profile and, based on several experimental tests, a standard basic mission profile is created. Long-term tests are carried out by repeating the proposed basic load profile. Yet, power transitions of the basic load profile are smoother than the real driving profile. Consequently, real performances might be far from long-term test results. In [41], the importance of hybridizing a fuel cell with an

energy storage unit is outlined. A fuel cell-battery active hybrid is designed for a lightweight AUV. The proposed design procedure is based on the energy balance, size and weight of the vessel under test. Yet, the cyclic load profile between two power levels is accounted for, which is really far from the actual working conditions of an AUV. Criteria for hydrogen storage methods are discussed. In [42], a review of the state of art of the hybrid power systems for propelling aerial vehicles based on the active coupling between fuel cells and batteries is presented. Several fuel cell technologies are accounted for. In [43], the importance of using a fuel cell in small ships and underwater vehicles because of its zero-emissions, low noise and high efficiency features is outlined. A 20 kW active hybrid system for small ships or AUVs based on PEMFC and lead acid batteries is proposed. Yet, a cyclic load profile is assumed. Experimental tests show that, if the stack is fed by pure oxygen instead of air, the PEMFC power will almost double.

This paper is focused on the design and implementation of an indirect hybrid fuel cell/battery power system for the propulsion of a prototype of ASV, called the Eco-SWAMP. The Eco-SWAMP is a fuel cell powered AMV which can be programmed or remotely controlled to follow a trajectory, namely a mission. The SWAMP prototype, powered by batteries, is firstly described. The Eco-SWAMP power supply system is designed and sized based on SWAMP experimental results. Power management algorithms are designed and tested. Simulation results in MATLAB/Simulink environment are shown to validate the efficiency of the proposed sizing procedure.

In section 2, the battery-powered prototype of the SWAMP vehicle is presented, including physical and geometrical parameters of the SWAMP AMV and the electrical ratings of installed batteries. In section 3, experimental results on the battery-powered SWAMP vehicle are shown. Experimental results on the power consumption profile of the SWAMP vehicle are required for the proposed sizing and power management algorithms to be implemented on the Eco-SWAMP. In Section 4, the sizing method for the Eco-SWAMP basic primary sources, based on SWAMP experimental results, is proposed and discussed in detail. In Section 5, power management algorithms are designed and validated by simulation results. In Section 6, conclusions are drawn.

2. The SWAMP: an autonomous marine vehicle prototype

SWAMP (Shallow Water Autonomous Multipurpose Platform) is a robotic solution targeted to answer the practical needs of monitoring the extremely shallow waters that are peculiar of Wetlands for a better acquisition of the environmental parameters. In this environment, robotic tools are intended to help human beings to improve the precision and the quality of the surveys and to perform tasks in those areas where the access is dangerous or difficult.

SWAMP is the first of a new class of modular, portable, lightweight, re-configurable ASVs for extremely shallow water and remote areas applications and it was built in the frame of a collaboration between CNR-INM and DITEN-Unige [2]. SWAMP is a double-ended catamaran that combines the ability of working in a few centimetres of water together with satisfactory control abilities. This is achieved thanks to the use of a four modular azimuth thruster based on Pump-Jet that are designed for extremely shallow waters. Moreover, to work in these areas, SWAMP is characterized by small draft soft-foam, unsinkable hull structure where all the elements are contained within the hulls in a protected impact resistant zone. The requirement of making different kinds of surveys demands for high modularity and a flexible hardware/software architecture. SWAMP architecture is based on an on-board Wi-Fi network that allows for easily integrating sensors and samplers. Fig.1 shows the SWAMP vehicle during a survey.

Fig. 1 - SWAMP vehicle during a survey with a payload box on the deck

SWAMP is a full-electric Catamaran 1.23 m long with a design breadth of 1.1 m. The hull height is 0.4 m and the vehicle with the structure and the antennas is 1.1 m high. SWAMP lightweight is 38 kg with a draft of 0.1 m. The reserve of buoyancy given by the soft-foam allows it to embark up to 60 kg with a draft of 0.22 m. SWAMP is composed of two mono-hulls that can be disassembled. Indeed one of the main peculiarities of SWAMP consists in the fact that each hull is conceived to be a single ASV with its propulsion units, navigation guidance and control unit (composed of an IMU and a GPS), communication and power system. This possibility is guaranteed by the existence of the above-mentioned Wi-Fi-based communication architecture. The communication is created by one communication module that is present in each hull that provides a communication framework for both its same hull and for the other hull's modules when its work is required. With this idea, the deck of the vehicle is free for hosting any payload, users and sensors, additional powering devices like fuel cells or solar PV panels, landing pads for drones and what else is required. SWAMP specifications are listed in Table 1.

Parameter	**Specification**		
Hull Type	Modular double-ended catamaran		
Overall Length	1230	[mm]	
Nominal Width	1100	[mm]	800-1250
Distance Between Hulls	800	[mm]	
Construction Height	500	[mm]	
Maximum Draft	150	[mm]	

Light Weight	38	[kg]	
Maximum Weight	60	[kg]	
Buoyancy Reserve	120	[kg]	
Autonomy	2	[h]	
Operating Speed	1	[kts]	
Maximum Speed	3	[kts]	
Battery Voltage	37	[V]	
Batteries	2	nr	1 each hull
360 deg Azimuth Thrusters	4 x 15	[N]	2 each hull
IMU	2	nr	1 each hull
GPS	2	nr	1 each hull
Cameras	2	nr	1 each hull

Table 1 – SWAMP specifications.

The vehicle is man-portable and transportable by car or in a small boat since the small dimensions of the vehicle comply with the idea of a reduced logistics. Each vehicle structure is composed of a light, soft and impact-survival flexible structure made with a sandwich of soft closed-cell foam, HDPE plates and pultruded bars. This flexible design allows hosting various types of tools, thrusters, control systems, samplers and sensors. As mentioned, the propulsion is based on modular Pump-Jet azimuth thrusters expressly designed and studied for shallow water ASVs [44]. With respect to classical Waterjet propulsion, the Pump-Jet is characterized by lower operative speeds, lower required draft and a structure flush with the hull that guarantees low impacting risk. The 360deg steer ability of the thruster guarantees a high manoeuvring ability in narrow spaces.

By using four Pump-Jet thrusters, as depicted in Fig. 2, the vehicle becomes highly controllable with the possibility of station keeping and path following together with a good redundancy that is also guaranteed by the presence of two different powering and controlling systems.

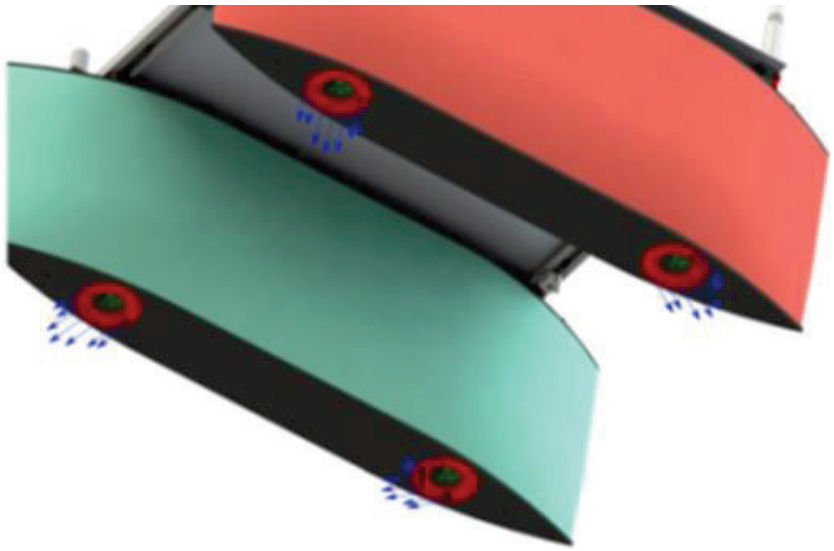

Fig. 2 - Thrust configuration and system

The hull is based on a double-ended wigley shape. This is not the optimum in terms of efficiency but allows finding a good match between conflicting requirements like lightness with a high payload, shallow draft, the need of hosting of the Pump-Jet thrusters, high controllability and a good endurance.

The hulls were tested in a towing tank both in deep water and in shallow water and this allowed us to find the curves of resistance for different immersions and payloads. Maximum speed of SWAMP in infinite depth waters at maximum payload is 1.6 m/s, while the speed in extremely shallow waters down to 200 mm (i.e. 60 mm of under-keel water) is reduced to 1 m/s due to the peculiar hydrodynamic effects occurring in shallow waters. Moreover, tests were performed in self-propelling condition and in bollard pull [45] in order to characterize the behaviour at speed of the Pump-Jet thrusters.

The results, given in form of resistance curves at different vehicle immersions, allow finding the increase in resistance given by the increase in payload. In this project, this is also used to understand how the increase in weight due to the use of FC increases the resistance of the vehicle.

Thanks to the above reported tests, it was then possible to dimension the required power and foresee various usage profiles of the SWAMP by means of the results obtained during the towing tank tests.

Each hull of SWAMP has its own powering pack with Lithium-ion Rechargeable cell batteries. Lithium-ion battery packs have a high round-trip efficiency and present lower volume, weight, temperature sensitivity and maintenance of lead-acid batteries. The choice has fallen on Li-ion, first of all for their lightness in relation to classical Lead acid Batteries.

Each watertight battery pack, weighing 3.2 kg, is composed of sets of cells with a voltage of 3.7 V and a capacity of 2.6 Ah. The batteries are composed of 10 batteries in series giving a resultant voltage of 37 V put in five parallel sets giving a resultant capacity of 13 Ah. Battery ratings are listed in Table 2.

Group	Parameter	Value	
Cells number	Series #	10	#
	Parallel #	5	#
Electrical characteristics	Nominal voltage	37	V
	Nominal capacity	13	Ah
	Energy	481	Wh
	Internal resistance	≤ 150 mΩ	
	Life cycles	> 800 cycles @ 1C 100% DOD	
	Monthly self-discharge	<3%	
	Charge Rate Relative Capacity efficiency	95% @ 0.5C	
	Discharge efficiency	99%	
	Peukert constant	1.0	k
	Depth of Discharge: DOD	95%	
	Depth of Discharge Limit	0.7	[Ah]
Standard charge	Charge voltage	42.0	V
	Charge mode	0.2C at 42V	
	Charge current	1 A	
	Maximum charge current	6 A	
	Charge limit voltage	42 +/- 0.1 V	
Discharge standard	Standard Disc. Capacity	12.75	Ah
	Direct current	10 A	
	Maximum current	15 A (<5min)	
	Discharge limit voltage	28	V
Environment	Charge temperature	0 ° C to 45 ° C @ 60 +/- 25% Relative humidity	
	Discharge temperature	-20 ° C to 60 ° C @ 60 +/- 25% Relative humidity	
	Storage temperature	0 ° C to 40 ° C @ 60 +/- 25% Relative humidity	
Physical characteristics	Humidity	5% ≤ RH ≤ 85%	
	Cell and Method	18650 / 10S5P	
	Plastic container	PVC	
	Dimension	mm 76 x 70 x 300 h	
Weight	Weight	3Kg	

Table 2 - Ratings of the SWAMP batteries.

The choice of the batteries was done with the idea of a minimum of endurance of 2 hours during the most critical mission and a maximum of 6 hours under a low power consumption. This depends on the usage of the SWAMP ASV and on the requirements of the mission. For shallow water, lower speeds are requested to maintain the endurance, a reduced mission shall be considered due to the higher resistance coefficients. Additional power batteries may easily be installed on board of SWAMP in case of higher power consumption, long missions or additional payloads that require a high on-board power.

Due to the on-board presence of various users running at various voltages, a series of industrial DC-DC converters had to be chosen. Depending on the current and power needs of the single devices. Users at 5V, 12V, 24V, 36V are on-board. From a list of these users, it was also possible to extract the power required by the entire system, considering the extreme case of operation at the maximum power of all the on board systems.

The vehicle sends its telemetry through its on-board communication system to the land station. The data comprise the usage of the thrusters and of the vehicle tools.

The data obtained from the four different missions were used to obtain the profiles of powering that can be required in standard future missions.

3. The power consumption profile of the AMV SWAMP

The power consumption profile during four missions is recorded and further investigated. The SWAMP is conceived as a black box and the power drawn from both batteries is recorded. The recorded power includes both the on-board electronic equipment and the propulsion power consumption. Experimental results on the SWAMP are collected to proceed towards a proper size of the primary energy sources of the Eco-SWAMP. The size procedure aims at defining ratings of the battery, the fuel cell and the on-board hydrogen reserve to complete the reference missions efficiently. Increasing the cruising range and lowering the environmental impact are the main goals of the Eco-SWAMP design. Dimension and weight constraints should be complied with.

Two reference cases were obtained during autonomously controlled missions in Biograd Na Moru (HR), the first during a testing on the functionality of SWAMP (MISSION C) that lasted 1h 30 min and the second during a bathymetric survey (MISSION B) lasted 5 h. Another case was obtained in Camogli (IT) during an experiment of citizen science where the vehicle was remotely controlled by operators to make a specified S-shape path (MISSION A) that lasted 6h. In this case, only two Pump-Jet motors were activated. The final case was obtained on the Roja River (IT) during a bathymetric survey where the vehicle was remotely controlled (MISSION D) that lasted 3h.

During the test cases, the vehicle was not equipped with all the instruments and all the users foreseen during the design (cameras, sonar, sensors). Since the higher consumption (up to 75%) comes from the propulsion system and the propulsion system has the most variable trend among users, in order to maximize the estimate of vehicle consumption with a realistic forecast of use, it was chosen to proceed as follows. The total power P_m for each mission is obtained as the sum of the power of the propulsion units $P_p(t)$ coming from the telemetry and a constant power consumption as the sum of the theoretical powering of all the other users P_u.

$$P_m = P_p(t) + P_u \tag{1}$$

By adopting these criteria, we could maximise the estimation of total power consumption by taking into consideration realistic cases with the real values of the variation of the propulsion unit; this is the main source of power consumption on SWAMP and mostly variable source of power consumptions. In Fig. 3, the experimental results are shown. Significant parameters are defined: the total time, which is equal to the mission duration, the peak power consumption and the average power consumption over the whole mission total time. These parameters are of key importance to size the primary energy sources of the Eco-SWAMP. Table 3 sums up the four missions' significant parameters. MISSION A fixes the cruising range of the Eco-SWAMP with its 6 hours of total time, the longest among the others. The minimum average power consumption is recorded during MISSION B, affecting the fuel cell power ratings depending on the proposed power management strategy. The maximum peak power consumption belongs to both MISSION C and D. The peak power consumption and the power

consumption waveform as well, i.e. the drawn energy to complete the mission, affect the battery capacity ratings. The total time, the power ratings of the fuel cell and the battery capacity affect the hydrogen reserve size, which is required to complete the programmed and remotely controlled missions.

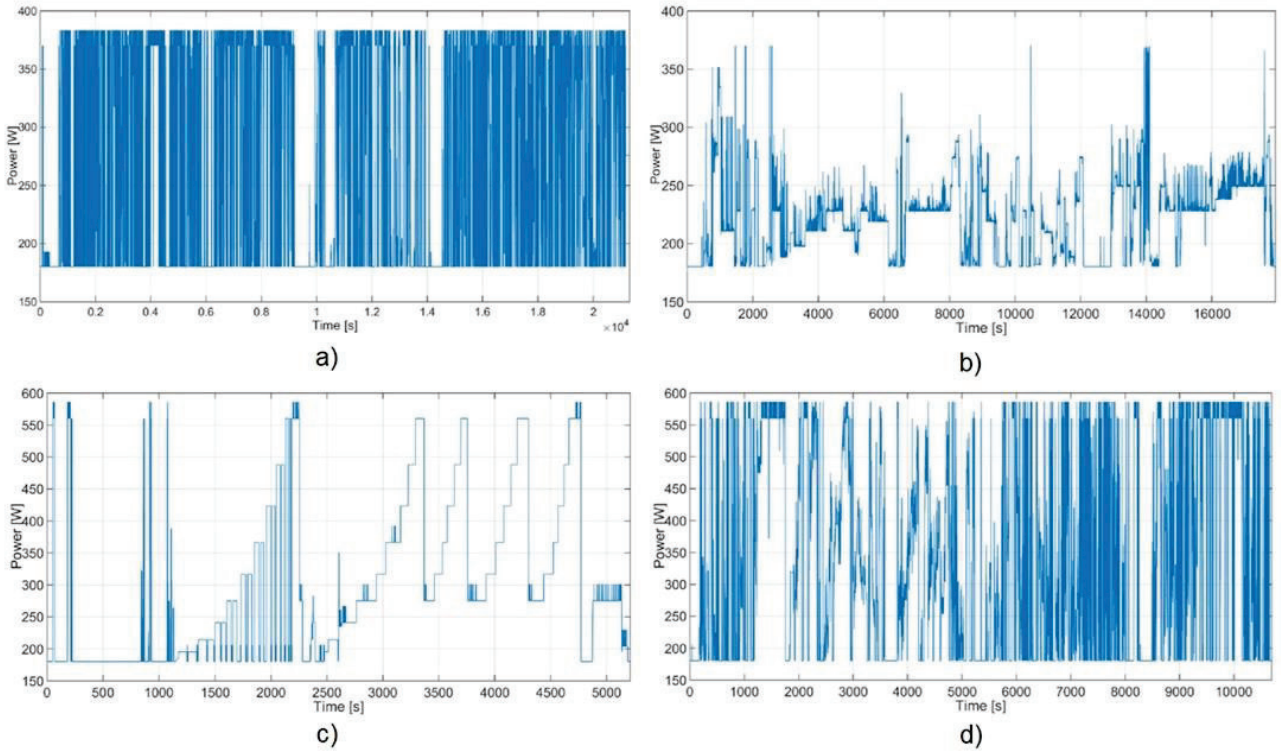

Fig. 3 - Experimental results during the four reference missions. Recorded power consumption profiles during MISSION A (a)), B (b)), C(c)) and D (d)).

Parameter	MISSION A	MISSION B	MISSION C	MISSION D
Total time	6h	5 h	1h 26m	3h
Average Power Consumption	271.64 W	221.14 W	295.52 W	329.32 W
Peak Power Consumption	383.2 W	370.2 W	586.2 W	586.2 W
Energy consumed	1621.2 Wh	1102Wh	427.7 Wh	978.2 Wh

Table 3 - List of significant parameters of the four reference missions.

4. Eco-SWAMP primary energy sources: size and ratings

The fuel cell power ratings depend on the adopted power management strategy. For the Eco-SWAMP, a load levelling technique is firstly proposed. According to the proposed strategy, the fuel cell equivalent load is kept constant as long as possible and the battery will source or sink the extra-power.

By implementing the load levelling, the risk for oxygen starvation and flooding can be efficiently avoided and the slow fuel cell transient response will not affect the dynamic performance of the whole power supply system. The Eco-SWAMP features a pulsed profile, with high peak power consumption and power slew-rate. Consequently, the fuel cell will supply the average power consumption whereas the battery will source or sink the extra-power. Therefore, the dynamic response of the whole power supply system depends on the battery performance whereas the single fill up (SFU) cruising range of the Eco-SWAMP depends on the fuel cell ratings and hydrogen reserve. The average power consumption ranges from 221.14 W (MISSION B) to 329.32 W (MISSION D). The fuel cell constant power is fixed at the minimum-recorded average power consumption to ensure that during the mission, on average, the battery will discharge. Consequently, the fuel cell power threshold is fixed at 220 W. By a market survey, the H-300 fuel cell, supplied by Horizon Fuel Cell Technologies Inc., featuring a 300 W nominal power is selected. The H-300 stack ratings are listed in Table 4. Even a power rating of 250 W could be selected. Yet, the conversion efficiency of a PEM fuel cell peaks at approximately 50% ÷ 56% at one-half of the nominal power and then it decays until the nominal power is reached. Therefore, the fuel cell is frequently working at half of the nominal power. Horizon Fuel Cell Technologies Inc. ensures a 40% efficiency value at the nominal power and therefore the H-300 PEM stack could be efficiently selected for the proposed application. The H-300 PEM stack can be supplied by a metal-hydride storage tank. Metal hydride hydrogen storage is actually the best choice for transport applications because of its low working pressure (maximum 30 bar) and safety concerns [46]. A metal-hydride storage tank featuring less than 2 L volume, weighing less than 7 Kg is required to comply with the Eco-SWAMP dimension and weight constraints. Therefore, by choosing a MyH2-900 cartridge by H2Planet supplier leads to a 900 L equivalent hydrogen storage. Dimensions are cylindrical with a 10 cm diameter and 38 cm height, fully compliant with the Eco-SWAMP dimension constraint. The tank weighs 6.9 Kg, fully compliant with the Eco-SWAMP payload constraint. The maximum H-300 hydrogen flow rate is equal to 3.9 L/m. Consequently, the fuel cell single-fill up (*SFU*) range can be obtained by Eq. (2).

$$SFU = \frac{900\ L}{3.9\ L/m} = 230.77\ m \equiv 13846\ s \equiv 3h\ 51m \quad (2)$$

Parameter	Value
Type of Fuel Cell	PEM
Number of cells	60
Rated Power	300 W
Performance	36 V @ 8.3 A
H2 supply valve voltage	12 V
Purging valve voltage	12 V
Reactants	Hydrogen and Air
External Temperature	5 to 30°C
Maximum Stack Temperature	65°C
H2 pressure	0.45 – 0.55 bar
Hydrogen Purity	≥99.995% dry H2
Humidification	Self-humidified
Cooling	Air (integrated cooling fan)
Stack weight (with fan and casing)	2790 g (±50 g)
Controller weight	400 g (±30 g)
Dimension	11.8 cm x 26.2 cm x 9.4 cm
Flow rate at maximum output	3.9 L/min
Start up time	≤30 s at ambient temperature
Efficiency of the stack	40% @ 36 V
Low voltage shut down	30 V
Over current shutdown	12 A
Over temperature shut down	65°C
External power supply	13 V ±1 V, 5 A

Table 4 - Ratings of the fuel cell selected for the Eco-SWAMP.

After selecting the fuel cell size and a metal-hydride storage tank, the battery capacity should be sized to complete all of four reference missions efficiently. The fuel cell SFU range together with the battery capacity will determine the SFU cruising range of the Eco-SWAMP.

Fig. 4 shows a drawing of the Eco-SWAMP prototype including the fuel cell stack and hydrogen cylinder.

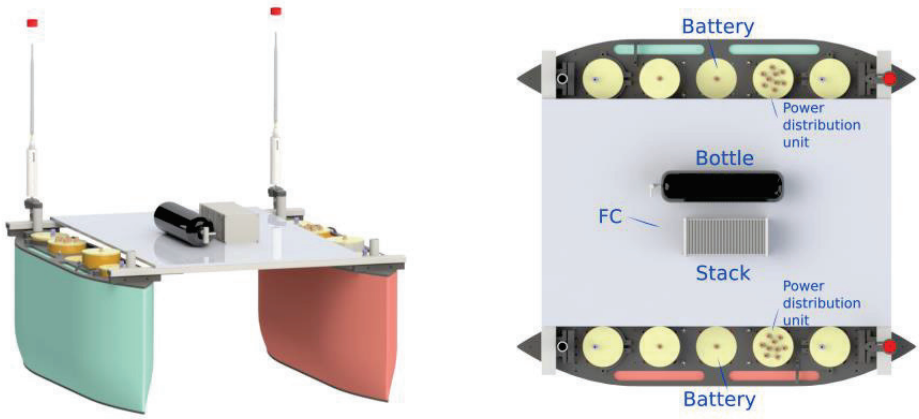

Fig. 4 - Drawing of the Eco-SWAMP

Vehicle endurance is a function of hydrodynamic resistance that influences the propulsion powering which indeed is the highest source of power consumption in the vehicle. Resistance (R) can be written as

$$R = \frac{1}{2}\rho W_s C_t U^2 \tag{3}$$

where ρ is density W_s is the static wetted surface, C_t is a resistance coefficient obtained from the towing tank tests and U is the vehicle speed. The resistance is then a function of the wetted surface, which is modified as the vehicle immersion increases or decreases. Therefore, the wetted surface is modified when the weight of the vehicle increases or decreases (Archimedes principle). The adoption of fuel cell will lead to a weight increase of about 6.2 kg that means that, in the first prototype of Eco-SWAMP, in order to compare the endurance with the one of the battery-powered vehicle, it is necessary to either reduce the embarked payload in addition to the fuel cell, or reduce the operative speed. Yet, for the operative part, if the payload is kept constant the total weight of the vehicle by adding the FC to the payload already considered needs to be increased. This causes an increase in resistance that will lead to a reduction in speed since the total force produced by the thrusters is limited. As shown in Fig. 5, the towing tank tests show that with an increase in maximum payload of 10 kg we have a not relevant 2% decrease in the maximum speed which remains above the maximum expected speed of 1.5m/s at the same maximum power. Figure 5 shows a 12% increase in propulsive powering at the maximum speed and a negligible increase at the cruising speed of 1 m/s. As shown

in Fig.5, there is no appreciable increase in resistance at operating speeds around 1 m/s. Consider that normal sampling operations are performed at this speed.

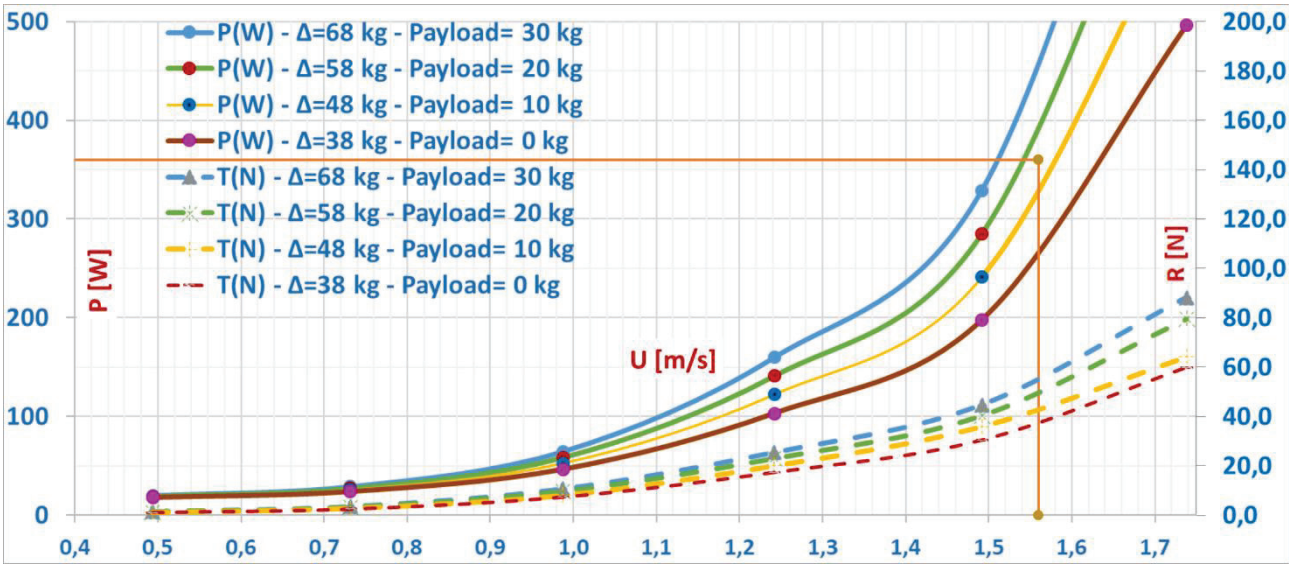

Fig. 5 – At the top, resistance curves in function of vehicle speed at different weights from 38 kg with 0 kg payload to 68 kg with 30 kg of payload are shown. At the bottom, powering curves in function of vehicle speed at different weights from 38 kg with 0 kg payload to 68 kg with 30 kg of payload are plotted.

A simulation model in MATLAB/Simulink environment is designed to size the required battery capacity. The designed value is indeed a minimum value for the battery capacity. Yet, the minimum value is here selected to comply with dimensions and weight constraints.

Fig.6 shows the MATLAB/Simulink model. The mission profile *Ptot* is derived from the experimentally recorded one by means of the "*From Workspace*" Library block. It is assumed that the fuel cell stack will supply a constant power of 220 W for 13846 s, which corresponds to the obtained SFU range of the fuel cell itself. After 13846 s, the fuel cell power decays to zero value. The difference between the total power *Ptot* and the fuel cell power, which is the output of the *switch* block, is equal to the extra-power, which will be sourced by the battery itself. By performing a signal integration, the battery energy is obtained, as well as the average battery power over the whole mission. Dividing the battery energy by its nominal voltage value, the battery capacity is obtained. In

Fig.7, simulation results under MISSION A (*a)*), B (*b)*), C (*c)*) and D (*d)*) are shown. On the top screen, the instantaneous value of the battery energy in Wh, is shown. The bottom screen shows the battery power in blue, the fuel cell power in red and the load power in yellow. After 13846 s from the mission start, the fuel cell power decays to zero value and the battery power will be equal to the load power.

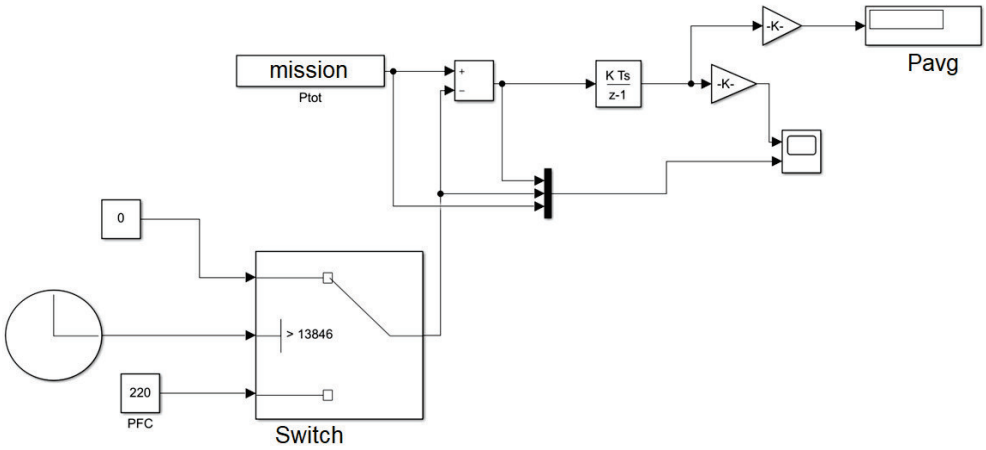

Fig. 6 - MATLAB/Simulink model for battery size.

Two different sizes are made with 48 V or 36 V nominal voltage value. Table 5 sums up size results. MISSION A burdens the battery with extreme load. The SWAMP is actually powered by two equal batteries, each featuring a 36 V nominal value and 13 Ah capacity. As shown from Table 4 data, a single battery is not adequate for MISSION A unless the fuel cell power threshold is shifted towards the stack nominal power of 300 W. Therefore, a single battery of the SWAMP prototype is chosen for the Eco-SWAMP design. Then, when the MISSION A is programmed, a 300 W power threshold will be selected in order to ensure a proper mission execution. Otherwise specified, a 220 W fuel cell power threshold is fixed.

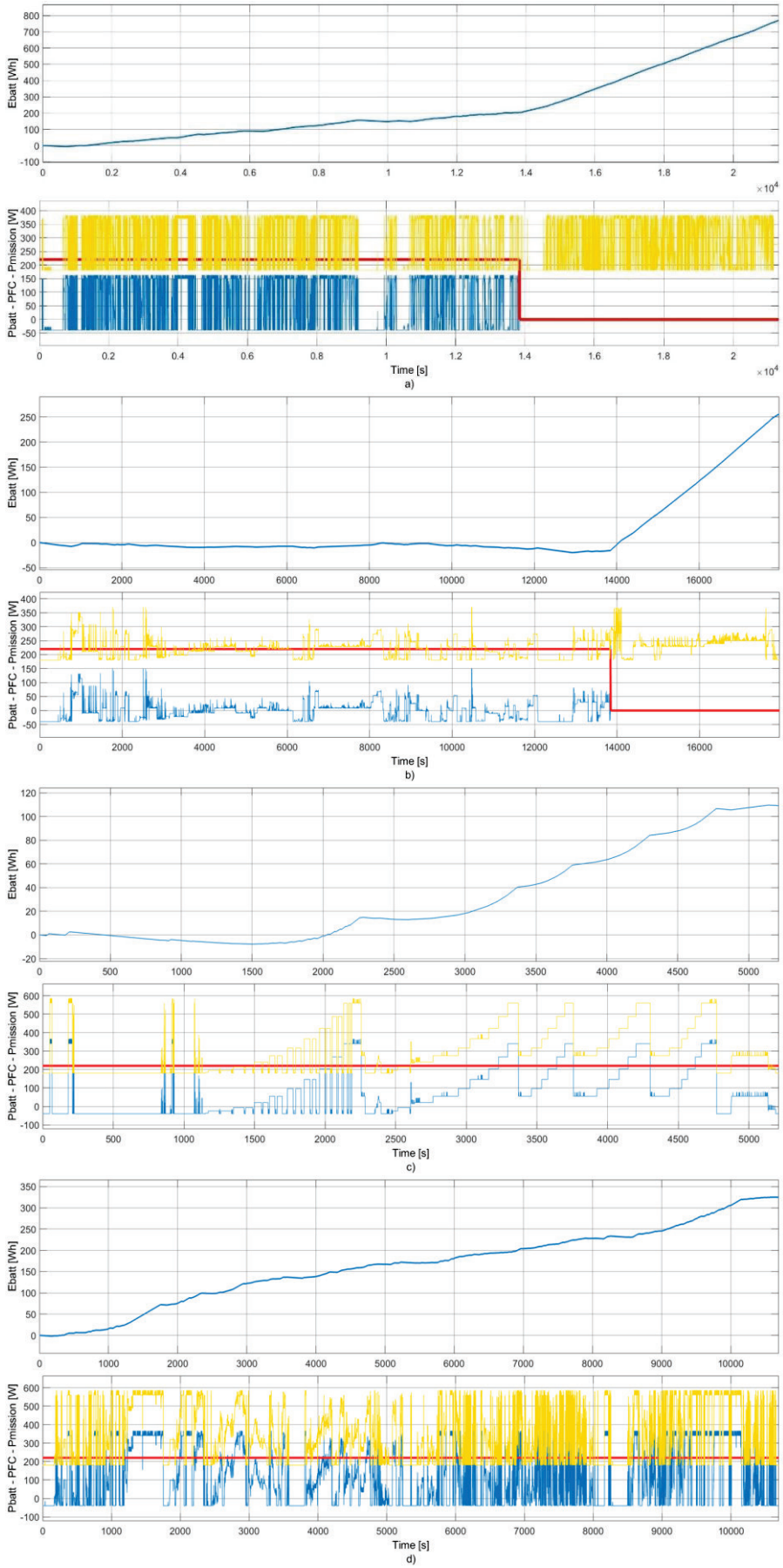

Fig. 7 - Simulation results during MISSION A (*a)*), B (*b)*), C (*c)*) and D (*d)*). The bottom screen of each subfigure shows the battery power in blue, the fuel cell power in red and the load power in yellow.

Mission	Cbatt (Vbatt=48 V)	Cbatt (Vbatt=36 V)
MISSION A (6h)	16 Ah (220W supplied by the FC) 9.6 Ah (300W supplied by the FC)	21.3 Ah (220W supplied by the FC) 12.8 Ah (300W supplied by the FC)
MISSION B (5h)	5.3 Ah (220W supplied by the FC)	7 Ah (220W supplied by the FC)
MISSION C (1h26m)	2.27 Ah (220W supplied by the FC)	3 Ah (220W supplied by the FC)
MISSION D (3h)	6.77 Ah (220W supplied by the FC)	9 Ah (220W supplied by the FC)

Table 5 - Required battery capacity for the Eco-SWAMP during the four reference missions.

5. Eco-SWAMP power managements algorithms

The front-end Eco-SWAMP power system architecture is based on a common DC bus. The fuel cell is interfaced to the common DC bus by a unidirectional DC-DC converter performing buck-boost conversion. The battery is interfaced to the common DC bus architecture by a bidirectional power converter ensuring efficient charge and discharge options. During the mission, the fuel cell could charge the battery according to the load power requirements. The proposed architecture is modular, thus featuring high design flexibility. If a renewable energy source is added to the power system, it will be connected to the common DC bus by means of a new interface converter. Thanks to the proposed modular architecture, the quota percentage of green energy could be increased by slightly modifying the power system configuration. In a near future, for ships and boats with less stringent constraints in terms of weight and dimensions, the hydrogen reserve will be generated on-board by means of photovoltaic sources, therefore increasing the quota percentage of on-board green energy. In the near future, the proposed method and on-board production could be implemented to the SWAMP mother-ship. Power management algorithms are designed and tested in MATLAB/Simulink environment. Two power management algorithms are analysed, namely PM1 and PM2. It is assumed that the battery could be charged by the fuel cell itself if its state of charge decays below 90% and the total load power consumption Pmission is less than the fuel cell power threshold PFC.

Based on these assumptions, if the total load power consumption is higher than the fuel cell power threshold, the fuel cell power will be limited to the power threshold value and the battery will source

the extra-power. If the total load power consumption is less than the fuel cell power threshold and the Battery State of Charge (SOC) is less than 90%, the fuel cell power will be limited to the power threshold and the battery will absorb the extra-power, thus charging. If Pmission<Pfc and the SOC is higher than 90%, the battery could not absorb the extra-power. Under these conditions, PM1 algorithm provides that the fuel cell will supply the power load while the battery keeps in rest, thus preserving its SOC. Under these conditions, the PM2 algorithm provides that the battery will supply the load and the fuel cell will be turned off thus saving hydrogen reserve. Power management algorithms flow charts of PM1 and PM2 are shown in Fig.8 and Fig.10, respectively.

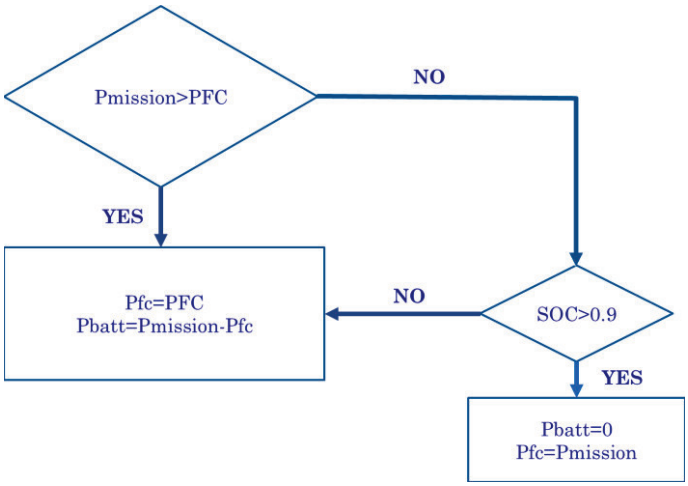

Fig. 8 - Flow chart of PM1 power management algorithm.

Fig.9 shows simulation results under the four reference missions and PM1 algorithm. For each subfigure, from the top to the bottom screen, the instantaneous fuel cell power *Pfc*, the instantaneous battery power *Pbatt*, the residual battery capacity *Cresidual* and the total load power profile *Mission* are shown. Under MISSION B, C, and D, the PM1 is highly efficient: a residual capacity is granted to the end of the mission. Under MISSION A, the residual capacity *Cresidual* reaches a zero value almost 30 minutes before the end of the mission. Therefore, according to preliminary simulation results, MISSION A cannot be efficiently completed. Further, the fuel cell power threshold is fixed at 300 W during MISSION A and 220 W during the others. The instantaneous fuel cell power *Pfc*

ranges from the instantaneous load power consumption to the power threshold value. After 13846 s from the mission start, the instantaneous fuel cell power *Pfc* decays to zero for fuel cell turn-off because of missing hydrogen reserve. During MISSION C and D, since the total time is less than 13846 s no fuel cell turn-off occurs. The battery sources or sinks the extra-power, as shown by simulation results. After 13846 s, when the fuel cell is turned-off due to the missing hydrogen reserve, the battery will entirely supply the on-board power load.

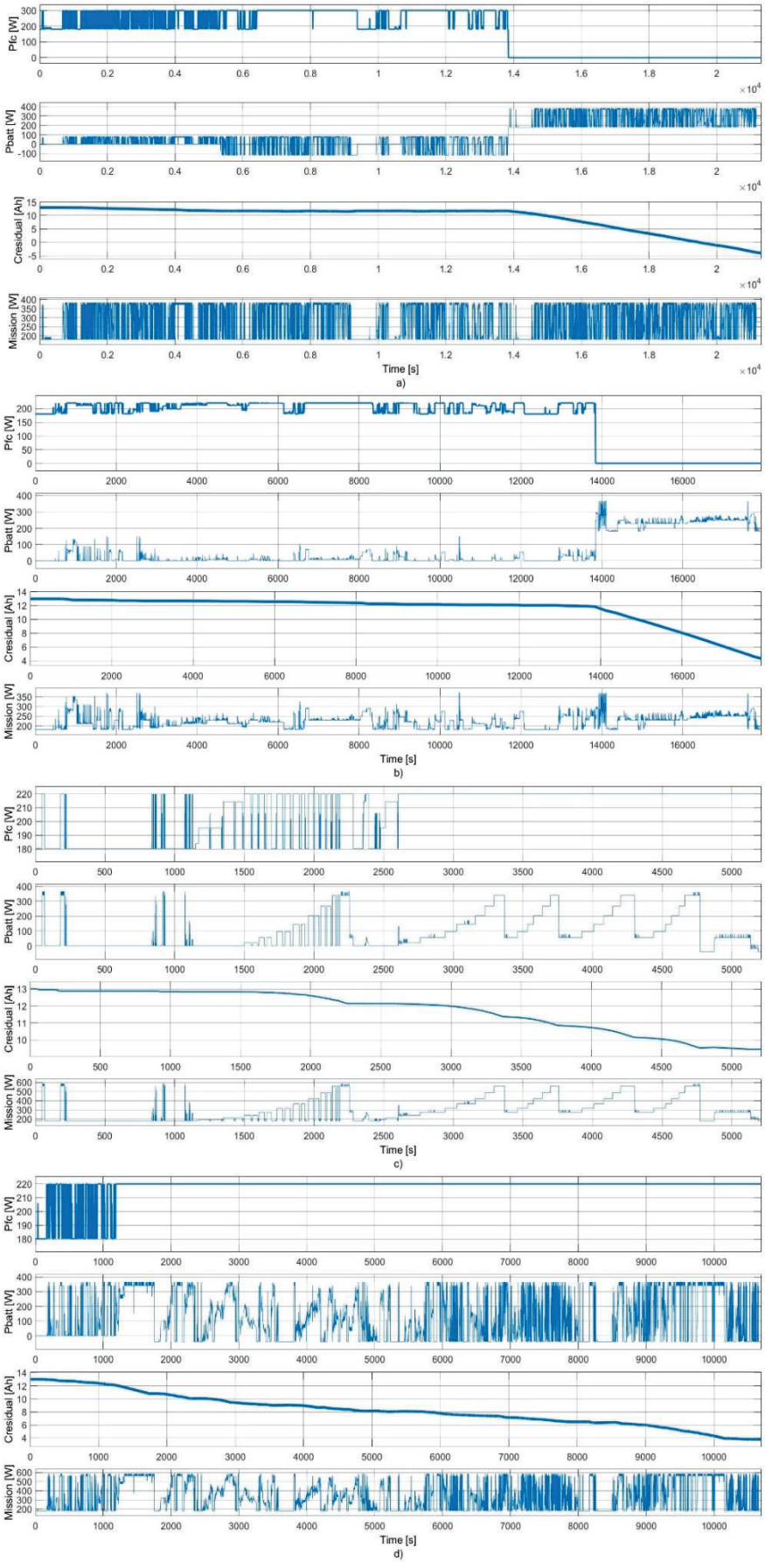

Fig. 9 - Simulation results under PM1 power management algorithms are shown. *a)* MISSION A results, *b)* MISSION B results, *c)* MISSION C results, *d)* MISSION D results.

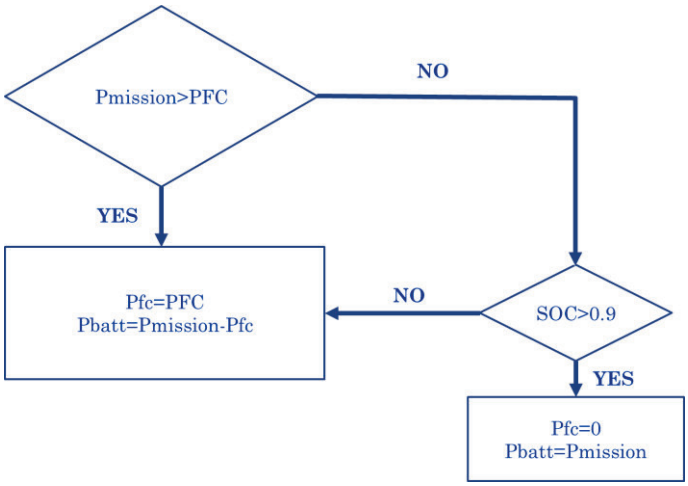

Fig. 10 - Flow chart of PM2 power management algorithm.

Fig.11 shows simulation results under the four reference missions and PM2 algorithm. For each, from the top to the bottom screen, the instantaneous fuel cell power *Pfc*, the instantaneous battery power *Pbatt*, the residual battery capacity *Cresidual* and the total load power profile *Mission* are shown. Under MISSION B, C, and D, the PM2 is highly efficient: a residual capacity is granted to the end of the mission. Under MISSION A, the residual capacity *Cresidual* reaches a zero value almost 30 minutes before the end of the mission. Therefore, according to simulation results, MISSION A cannot be efficiently completed. Further, the fuel cell power threshold is fixed at 300 W during MISSION A and 220 W during the others. The instantaneous fuel cell power *Pfc* ranges from zero to the power threshold value. Consequently, under the PM2 algorithm the fuel cell power commutation is 300 W - wide during MISSION A and 220 W during the other missions. Fuel cell power commutations are higher than under PM1. After 13846 s from the mission start, the instantaneous fuel cell power *Pfc* decays to zero for fuel cell turn-off because of missing hydrogen reserve. During MISSION C and D, no fuel cell turn-off occurs because the total time is less than 13846 s. The battery sources or sinks the extra-power, as shown by simulation results. After 13846 s, when the fuel cell is turned-off due to the missing hydrogen reserve, the battery will entirely supply the on-board power load.

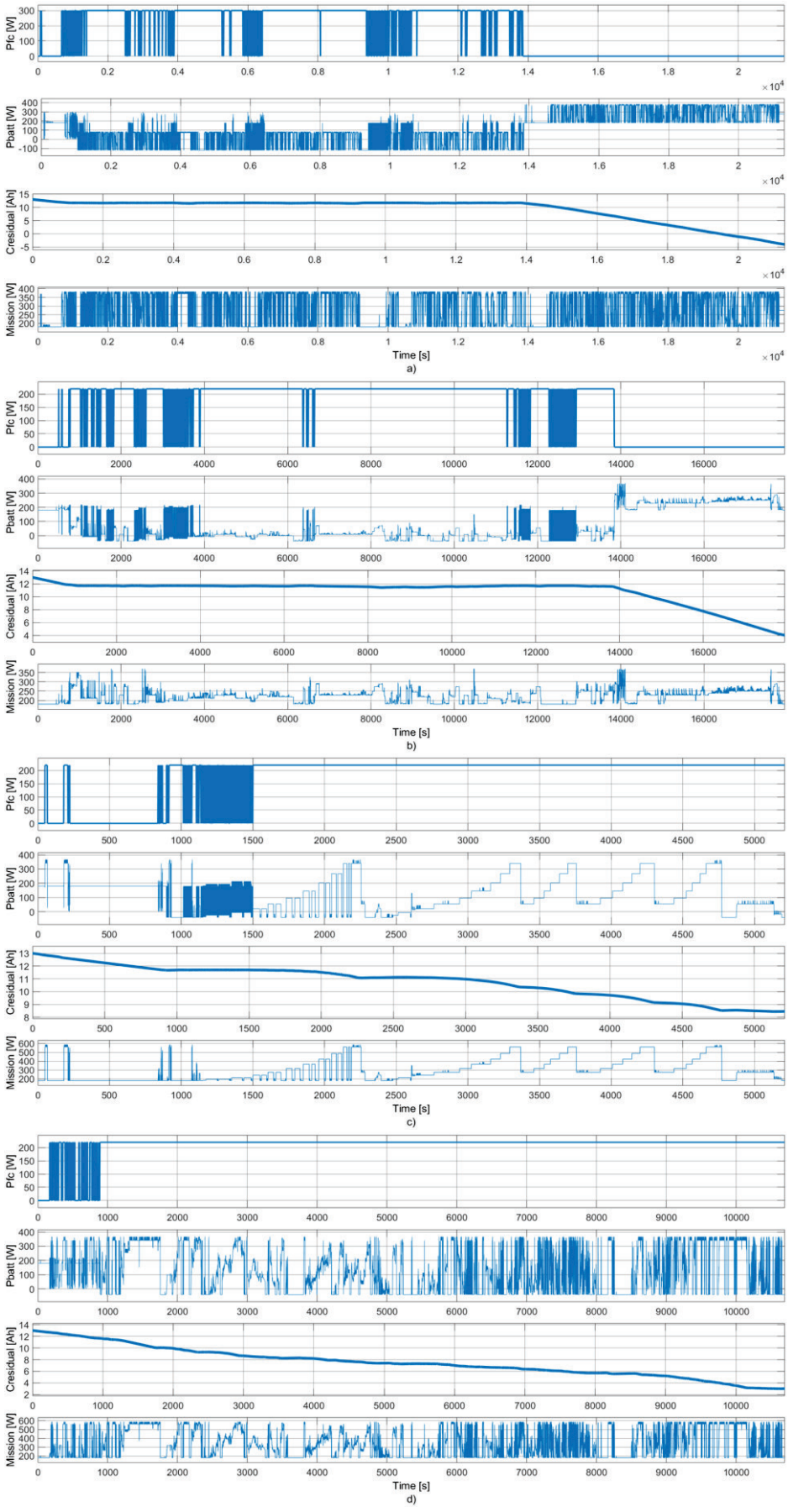

Fig. 11 - Simulation results under PM2 power management algorithms are shown. *a)* MISSION A results, *b)* MISSION B results, *c)* MISSION C results, *d)* MISSION D results.

Table 6 sums up the simulation results during the four reference missions. As shown by simulation results, MISSION A cannot be completed efficiently with a 13 Ah battery. A more precise evaluation of the single fill up cruising range is required to validate the efficiency of the proposed algorithms during MISSION A.

MISSION	Parameter	PM1	PM2
MISSION A			
	Required $C_{residual}$	17 Ah	17 Ah
	Turn-off	30 m	30 m
MISSION B			
	$C_{residual}$	4.322 Ah	4.052 Ah
	% di C_{batt}	33 %	31 %
MISSION C			
	$C_{residual}$	9.458 Ah	8.449 Ah
	% di C_{batt}	72.75 %	65 %
MISSION D			
	$C_{residual}$	3.771 Ah	3.016 Ah
	% di C_{batt}	29 %	23.2 %

Table 6 - Simulation results during the four reference missions, PM1 and PM2 power management algorithms.

Note that, under PM2 fuel cell power commutation is wider than under PM1 because under PM2 the fuel cell is frequently turned-off. Even if the performances under both algorithms are almost the same, the PM1 algorithm is preferred in order to avoid the risk of flooding and oxygen starvation and protect the fuel cell from frequent start-up phases. PM1 will be considered for a more precise evaluation of the SFU cruising range of the Eco-SWAMP during MISSION A.

An energy balance computation is provided. The energy required to complete MISSION A is equal to 1621.2 Wh, as shown by simulation results. The battery, featuring a nominal voltage of 36 V and a capacity of 13 Ah, could source 468 Wh, obtained as the product of the nominal voltage and rated capacity. The fuel cell should supply 1153.2 Wh to complete MISSION A. By assuming that the fuel cell stack supplies 300 W over the whole turning-on period, the fuel cell would be able to supply 1153.8 Wh, which is higher than the required energy. Instead of turning off the fuel cell after 13846s from the mission start, the fuel cell turn-off is forced after the supplied energy overcomes the 1153.8 Wh threshold. The model has been modified accordingly. Consequently, the model has been updated

to account for variable fuel cell power. The new model is more precise in terms of accuracy in determining the fuel cell turn-off instant.

Fig.12 shows simulation results with the updated model during MISSION A under PM1 algorithm. From the top to the bottom screen, the instantaneous fuel cell power *Pfc*, the instantaneous battery power *Pbatt*, the residual battery capacity *Cresidual* and the total load power profile *Mission* are shown. As shown by simulation results, the fuel cell turns-off after 4 h 28 m from the mission start. The fuel cell cruising range is higher with the updated model. Under these conditions, even the MISSION A is completed efficiently under the PM1 power management algorithm.

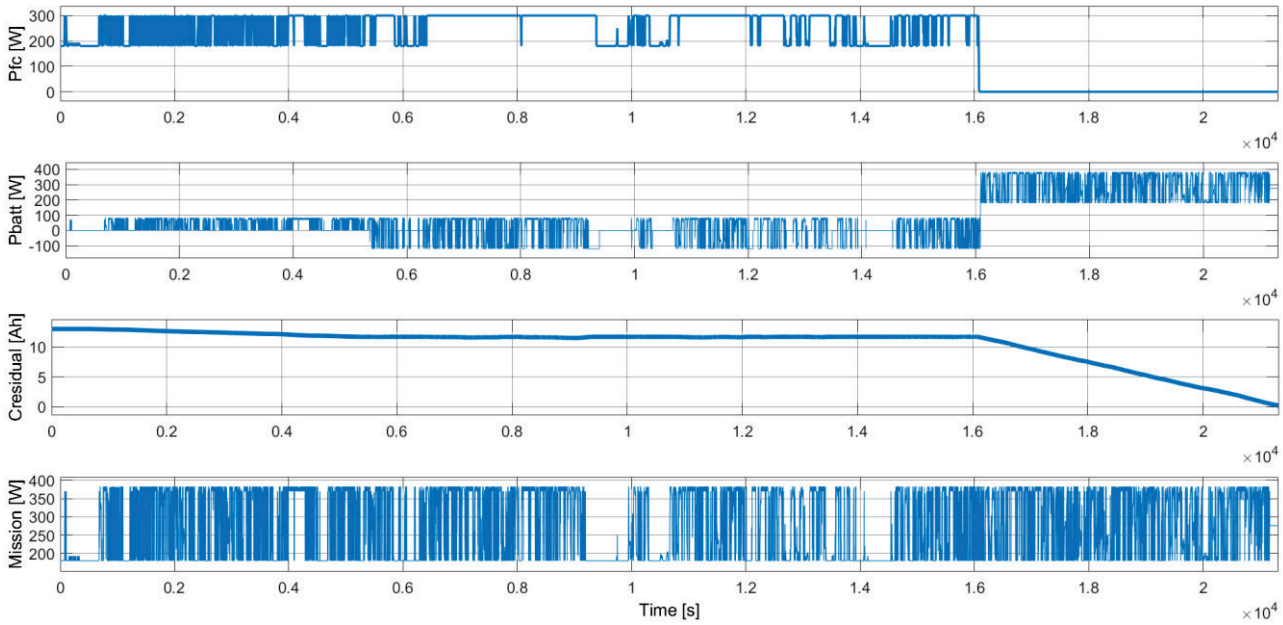

Fig. 12 - Simulation results under PM1 algorithm during MISSION A, according to the energy balance computation of the fuel cell cruising range.

As shown by simulation results, all Eco-SWAMP reference missions are efficiently completed in the proposed configuration: one battery with rated 36 V nominal voltage and 13 Ah rated capacity, a H-300 fuel cell stack with one on-board metal hydride hydrogen storage tank MyH2-900 and PM1 power management algorithm. According to simulation results, the SFU cruising range of the Eco-SWAMP is equal to 6 hours during the most crucial mission (MISSION A). The battery powered SWAMP actually features a 2 hours cruising range with the most critical pattern, according to experimental results. Instead of using two identical batteries, in the Eco-SWAMP one battery is

replaced by the fuel cell stack and hydrogen reserve. The new configuration gains 4 hours of cruising range. The new configuration complies with the Eco-SWAMP dimensions and weight constraints.

6. Conclusions

In this paper the design of a fuel cell powered autonomous surface vehicle, the Eco-SWAMP, has been presented. In order to increase the cruising range meanwhile lowering the environmental impact of the vehicle itself, a new energy configuration is designed and tested based on the experimental results of the battery-powered SWAMP prototype. A fuel cell stack with its metal hydride hydrogen storage tank has replaced one of the SWAMP batteries. The novelty in the prototype lies in supplying an extremely light weight ASV with stringent constraints in terms of cost, size and weight by means of a fuel cell with its own hydrogen reserve. Besides all the advantages brought by the fuel cell, cost, size and weight are usually weak points of the fuel cells. Thanks to the proposed sizing and power management algorithm, the fuel cell and its hydrogen reserve fit the Eco-SWAMP constraints. Starting from experimental results and characterization of the battery-powered SWAMP ASV prototype, a method for basic sources sizing of the Eco-SWAMP has been proposed. Four experimental reference missions (namely MISSION A, B, C and D) have been selected because of their critical state in terms of endurance, peak or average power consumption. Existing software usually outputs a specific design of physical, geometrical and chemical properties of the stack itself to improve system performances. In this paper, fuel cell ratings as well as battery ratings have been fixed thanks to the proposed method under weight, size and volume constraints dictated by the SWAMP prototype. The proposed method accounts for compliance with physical and geometrical constraints of the specific application and therefore shortens the time to market and the gap between simulation and experimental results. Two power management algorithms, namely PM1 and PM2, have been designed and compared to solve the trade-off between the size, power ratings, volume and weight of the hybrid power supply. As shown by simulation results in MATLAB/Simulink environment, both algorithms show adequate performances in terms of endurance and dynamic response of the hybrid power supply, leading to compliance with physical and geometrical

constraints. Yet, PM1 has been selected in order to increase the service life of the on-board fuel cell stack. Six hours of cruising range under the most critical mission (MISSION A) have been granted by the proposed sizing method and power management algorithm. As shown by simulation results, the proposed configuration of the Eco-SWAMP has gained 4 hours of cruising range with respect to the battery-powered SWAMP prototype. The proposed procedure can be easily applied to any autonomous surface marine vehicle, independently of the power ratings of the vehicle itself. For future developments, the Eco-SWAMP prototype will be tested to validate the proposed procedure.

7. Acknowledgements

Authors want to thank the technical staff composed by Marco Bibuli, Gabriele Bruzzone, Giorgio Bruzzone, Mauro Giacopelli, Edoardo Spirandelli and Enrica Zereik for their contribution in the design, construction and testing of the mechanical and electrical systems of the robotic platform.

The research was supported by the Italian National Research Program PON «Ricerca e Innovazione» 2014-2020 - Action II.2, Specialization area: "Blue Growth", Project n. ARS01_00682, Project acronym: ARES, Project title: Autonomous Robotics for the Extended Ship.

8. References

[1] d'Amore-Domenech R, Raso MA, Villalba-Herreros A, Santiago Ó, Navarro E, Leo TJ. Autonomous underwater vehicles powered by fuel cells: Design guidelines. Ocean Eng 2018;153:387–98. https://doi.org/https://doi.org/10.1016/j.oceaneng.2018.01.117.

[2] Odetti A, Bruzzone G, Altosole M, Viviani M, Caccia M. SWAMP, an Autonomous Surface Vehicle expressly designed for extremely shallow waters. Ocean Eng 2020;216:108205. https://doi.org/https://doi.org/10.1016/j.oceaneng.2020.108205.

[3] Bruzzone G, Odetti A, Caccia M, Ferretti R. Monitoring of Sea-Ice-Atmosphere Interface in the Proximity of Arctic Tidewater Glaciers: The Contribution of Marine Robotics. Remote Sens 2020;12. https://doi.org/10.3390/rs12111707.

[4] Zappalà G, Bruzzone G, Caruso G, Azzaro M. Development of an automatic sampler for extreme polar environments: first in situ application in Svalbard Islands. Rend Lincei

2016;27:251–9. https://doi.org/10.1007/s12210-016-0539-1.

[5] Specht C, Świtalski E, Specht M. Application of an autonomous/unmanned survey vessel (ASV/USV) in bathymetric measurements. Polish Marit Res 2017;24:36–44.

[6] Ferreira H, Almeida C, Martins A, Almeida J, Dias N, Dias A, et al. Autonomous bathymetry for risk assessment with ROAZ robotic surface vehicle. Ocean. 2009-EUROPE, 2009, p. 1–6. https://doi.org/10.1109/OCEANSE.2009.5278235.

[7] Caccia M, Bibuli M, Bono R, Bruzzone G, Spirandelli E. Unmanned Surface Vehicle for Coastal and Protected Waters Applications: the Charlie Project. Mar Technol Soc J 2007;41:62–71.

[8] Galceran E, Campos R, Palomeras N, Ribas D, Carreras M, Ridao P. Coverage Path Planning with Real-time Replanning and Surface Reconstruction for Inspection of Three-dimensional Underwater Structures using Autonomous Underwater Vehicles. J F Robot 2015;32:952–83. https://doi.org/https://doi.org/10.1002/rob.21554.

[9] Stanghellini G, Del Bianco F, Gasperini L. OpenSWAP, an Open Architecture, Low Cost Class of Autonomous Surface Vehicles for Geophysical Surveys in the Shallow Water Environment. Remote Sens 2020;12. https://doi.org/10.3390/rs12162575.

[10] Osen OL, Sandvik R, Berge Trygstad J, Rogne V, Zhang H. A novel low cost ROV for aquaculture application. Ocean. 2017 - Anchorage, 2017, p. 1–7.

[11] Mayer L, Jakobsson M, Allen G, Dorschel B, Falconer R, Ferrini V, et al. The Nippon Foundation—GEBCO Seabed 2030 Project: The Quest to See the World's Oceans Completely Mapped by 2030. Geosciences 2018;8. https://doi.org/10.3390/geosciences8020063.

[12] Vasilijevic A, Buxton B, Sharvit J, Stilinovic N, Nad D, Miskovic N, et al. An ASV for coastal underwater archaeology: The Pladypos survey of Caesarea Maritima, Israel. Ocean. 2015 - Genova, 2015, p. 1–7. https://doi.org/10.1109/OCEANS-Genova.2015.7271495.

[13] Allotta B, Costanzi R, Ridolfi A, Colombo C, Bellavia F, Fanfani M, et al. The ARROWS

project: adapting and developing robotics technologies for underwater archaeology. IFAC-PapersOnLine 2015;48:194–9. https://doi.org/https://doi.org/10.1016/j.ifacol.2015.06.032.

[14] Ferretti R, Bibuli M, Caccia M, Chiarella D, Odetti A, Ranieri A, et al. Towards Posidonia Meadows Detection, Mapping and Automatic recognition using Unmanned Marine Vehicles. IFAC-PapersOnLine 2017;50:12386–91. https://doi.org/https://doi.org/10.1016/j.ifacol.2017.08.2504.

[15] A. Mendez T. J. Leo, Herreros MA. Current State of Technology of Fuel Cell Power Systems for Autonomous Underwater Vehicles. Energies 2014;7:4676–93.

[16] Wang X, Shang J, Luo Z, Tang L, Zhang X, Li J. Reviews of power systems and environmental energy conversion for unmanned underwater vehicles. Renew Sustain Energy Rev 2012;16:1958–70. https://doi.org/https://doi.org/10.1016/j.rser.2011.12.016.

[17] Weydahl H, Gilljam M, Lian T, Johannessen TC, Holm SI, Hasvold JØ. Fuel cell systems for long-endurance autonomous underwater vehicles – challenges and benefits. Int J Hydrog Energy 2020;45:5543–53. https://doi.org/https://doi.org/10.1016/j.ijhydene.2019.05.035.

[18] Hasvold Ø, Størkersen NJ, Forseth S, Lian T. Power sources for autonomous underwater vehicles. J Power Sources 2006;162:935–42. https://doi.org/https://doi.org/10.1016/j.jpowsour.2005.07.021.

[19] Armand M, Axmann P, Bresser D, Copley M, Edström K, Ekberg C, et al. Lithium-ion batteries – Current state of the art and anticipated developments. J Power Sources 2020;479:228708. https://doi.org/https://doi.org/10.1016/j.jpowsour.2020.228708.

[20] Sabihuddin S, Kiprakis AE, Mueller M. A Numerical and Graphical Review of Energy Storage Technologies. Energies 2015;8:172–216. https://doi.org/10.3390/en8010172.

[21] Han G, Kwon Y, Kim JB, Lee S, Bae J, Cho E, et al. Development of a high-energy-density portable/mobile hydrogen energy storage system incorporating an electrolyzer, a metal hydride and a fuel cell. Appl Energy 2020;259:114175. https://doi.org/https://doi.org/10.1016/j.apenergy.2019.114175.

[22] Hasvold Ø, Størkersen N. Electrochemical power sources for unmanned underwater vehicles used in deep sea survey operations. J Power Sources 2001;96:252–8. https://doi.org/https://doi.org/10.1016/S0378-7753(00)00685-6.

[23] Coppola T, Micoli L, Turco M. State of the Art of High Temperature Fuel Cells in Maritime Applications. 2020 Int. Symp. Power Electron. Electr. Drives, Autom. Motion, 2020, p. 430–5. https://doi.org/10.1109/SPEEDAM48782.2020.9161898.

[24] Madsen RT, Klebanoff LE, Caughlan SAM, Pratt JW, Leach TS, Appelgate TB, et al. Feasibility of the Zero-V: A zero-emissions hydrogen fuel-cell coastal research vessel. Int J Hydrogen Energy 2020;45:25328–43. https://doi.org/https://doi.org/10.1016/j.ijhydene.2020.06.019.

[25] de-Troya JJ, Álvarez C, Fernández-Garrido C, Carral L. Analysing the possibilities of using fuel cells in ships. Int J Hydrogen Energy 2016;41:2853–66. https://doi.org/https://doi.org/10.1016/j.ijhydene.2015.11.145.

[26] Kim T, Kwon S. Design and development of a fuel cell-powered small unmanned aircraft. Int J Hydrog Energy 2012;37:615–22. https://doi.org/https://doi.org/10.1016/j.ijhydene.2011.09.051.

[27] Shih N-C, Weng B-J, Lee J-Y, Hsiao Y-C. Development of a small fuel cell underwater vehicle. Int J Hydrog Energy 2013;38:11138–43. https://doi.org/https://doi.org/10.1016/j.ijhydene.2013.01.095.

[28] Maeda T, Ishiguro S, Yokoyama K, Hirokawa K, Hashimoto A, Okuda Y, et al. Development of Fuel Cell AUV" URASHIMA. Mitsubishi Heavy Ind Tech Rev 2004;41:344–7.

[29] Bethoux O. Hydrogen Fuel Cell Road Vehicles: State of the Art and Perspectives. Energies 2020;13. https://doi.org/10.3390/en13215843.

[30] Fletcher T, Ebrahimi K. The Effect of Fuel Cell and Battery Size on Efficiency and Cell Lifetime for an L7e Fuel Cell Hybrid Vehicle. Energies 2020;13.

https://doi.org/10.3390/en13225889.

[31] Veziroglu A, Macario R. Fuel cell vehicles: State of the art with economic and environmental concerns. Int J Hydrogen Energy 2011;36:25–43. https://doi.org/https://doi.org/10.1016/j.ijhydene.2010.08.145.

[32] Hornfeld W. DeepC: The New Deep Water AUV Generation. vol. Volume 3:, 2003, p. 713–21. https://doi.org/10.1115/OMAE2003-37358.

[33] Amamou AA, Kelouwani S, Boulon L, Agbossou K. A Comprehensive Review of Solutions and Strategies for Cold Start of Automotive Proton Exchange Membrane Fuel Cells. IEEE Access 2016;4:4989–5002. https://doi.org/10.1109/ACCESS.2016.2597058.

[34] Caisheng Wang, Nehrir MH, Shaw S. Dynamic models and model validation for PEM fuel cells using electrical circuits. IEEE Power Eng. Soc. Gen. Meet. 2005, 2005, p. 2115 Vol. 3-. https://doi.org/10.1109/PES.2005.1489284.

[35] Zimmermann T, Keil P, Hofmann M, Horsche MF, Pichlmaier S, Jossen A. Review of system topologies for hybrid electrical energy storage systems. J Energy Storage 2016;8:78–90. https://doi.org/https://doi.org/10.1016/j.est.2016.09.006.

[36] Cai Q.; Browning DJ. BDJ. BNP. Hybrid fuel cell/battery power systems for underwater vehicles. Proc. 3rd SEAS DTC Tech. Conf., 2008.

[37] Han K, Qian H, Zhang Q, Liu L, Hu X. Optimization of Energy Management System for Fuel-Cell/Battery Hybrid Power in Unmanned Aerial Vehicle. 2019 22nd Int. Conf. Electr. Mach. Syst., 2019, p. 1–6. https://doi.org/10.1109/ICEMS.2019.8921655.

[38] Chiche A, Lagergren C, Lindbergh G, Stenius I. Sizing the energy system on long-range AUV. 2018 IEEE/OES Auton. Underw. Veh. Work., 2018, p. 1–6. https://doi.org/10.1109/AUV.2018.8729812.

[39] Wang H, Zhang Y, Li H. Design of small usv power system based on hybrid storage of wind and light storage. 2019 5th Int. Conf. Transp. Inf. Saf., 2019, p. 532–6. https://doi.org/10.1109/ICTIS.2019.8883724.

[40] López González E, Sáenz Cuesta J, Vivas Fernandez FJ, Isorna Llerena F, Ridao Carlini MA, Bordons C, et al. Experimental evaluation of a passive fuel cell/battery hybrid power system for an unmanned ground vehicle. Int J Hydrog Energy 2019;44:12772–82. https://doi.org/https://doi.org/10.1016/j.ijhydene.2018.10.107.

[41] Cai Q, Brett DJL, Browning D, Brandon NP. A sizing-design methodology for hybrid fuel cell power systems and its application to an unmanned underwater vehicle. J Power Sources 2010;195:6559–69. https://doi.org/https://doi.org/10.1016/j.jpowsour.2010.04.078.

[42] Wang B, Zhao D, Li W, Wang Z, Huang Y, You Y, et al. Current technologies and challenges of applying fuel cell hybrid propulsion systems in unmanned aerial vehicles. Prog Aerosp Sci 2020;116:100620. https://doi.org/https://doi.org/10.1016/j.paerosci.2020.100620.

[43] Shih N-C, Weng B-J, Lee J-Y, Hsiao Y-C. Development of a 20 kW generic hybrid fuel cell power system for small ships and underwater vehicles. Int J Hydrog Energy 2014;39:13894–901. https://doi.org/https://doi.org/10.1016/j.ijhydene.2014.01.113.

[44] Odetti A, Altosole M, Bruzzone G, Caccia M, Viviani M. Design and Construction of a Modular Pump-Jet Thruster for Autonomous Surface Vehicle Operations in Extremely Shallow Water. J Mar Sci Eng 2019;7:222. https://doi.org/10.3390/jmse7070222.

[45] Odetti A, Altosole M, Bibuli M, Bruzzone G, Caccia M, Viviani M. Advance Speed-Hull-Pump-Jet Interactions in Small ASV, 2020. https://doi.org/10.3233/PMST200043.

[46] Bellosta von Colbe J, Ares J-R, Barale J, Baricco M, Buckley C, Capurso G, et al. Application of hydrides in hydrogen storage and compression: Achievements, outlook and perspectives. Int J Hydrogen Energy 2019;44:7780–808. https://doi.org/https://doi.org/10.1016/j.ijhydene.2019.01.104.